Supporting Information

Zeebe 10.1073/pnas.1222843110

SI Text

Equilibrium and Transient Response

The feedback analysis (starting with Eq. **1**) and the formulation of time-dependent climate sensitivity is based on a linearization around an initial equilibrium state (say global mean surface temperature T_0) and assumes that, under a sustained forcing, a new equilibrium will be established at $T_0 + \Delta T$. However, the transient response to establish this new equilibrium may take a long time, during which the system is not in equilibrium (e.g., Fig. 2*B*). Note that this type of behavior is not limited to the present case (e.g., ref. 1). The system's response time is governed by the sum of the feedbacks and the effective thermal inertia of the system (here, mostly ocean heat uptake; included in the projections; see below). Thus, the feedback analysis and the formulation of time-dependent climate sensitivity as presented here is not limited to equilibrium states. Rather, the transient response can be explicitly modeled, provided that the system's thermal inertia can be determined, as is the case here.

Long-Term Ocean–Atmosphere–Sediment CArbon Cycle Reservoir Model

The Long-term Ocean-atmosphere-Sediment CArbon cycle Reservoir (LOSCAR) model computes the partitioning of carbon between ocean, atmosphere, and sediments on timescales ranging from centuries to millions of years (2, 3). LOSCAR couples ocean–atmosphere routines to a computationally efficient sediment module. This allows, for instance, adequate computation of $CaCO_3$ dissolution, calcite compensation, and long-term carbon cycle fluxes, including weathering of carbonate and silicate rocks. The ocean component includes biogeochemical tracers such as total carbon, alkalinity, phosphate, oxygen, and stable carbon isotopes. LOSCAR's configuration of ocean geometry is flexible and allows for easy switching between modern and paleo-versions. We have previously published various tests and applications of the model tackling future projections of ocean chemistry and weathering, $p\mathrm{CO_2}$ sensitivity to carbon cycle perturbations throughout the Cenozoic, and carbon/calcium cycling during the Paleocene–Eocene Thermal Maximum (2–9). The model's architecture, its components, tuning, and examples of input and output are described in detail in ref. 3.

Uncertainties in Parameterizations. Several parameterizations were included in the LOSCAR model for the present study, which are subject to uncertainties (see below). For the most part, however, the uncertainties are not critical because they apply equally to projections that include and exclude slow feedbacks. The main point of this study is the difference between these two types of simulations (Fig. 2). Uncertainties in the slow feedbacks themselves are examined by varying the slow-feedback parameters (Fig. 3).

Greenhouse Gas Forcing. The global mean surface warming was calculated as:

$$\Delta T = S(t)(\Delta R_{\mathrm{CO_2}} + \Delta R_{\mathrm{CH_4}} + \Delta R_{\mathrm{N_2O}}), \qquad \textbf{[S1]}$$

where ΔR_n is the change in radiative forcing of greenhouse gas (GHG) n at atmospheric concentration C_n (10):

$$\begin{aligned} R_{\mathrm{CO_2}} &= 5.35\ \ln\left([\mathrm{CO_2}]/[\mathrm{CO_2}]_0\right) \\ &= 3.7\ \ln\left([\mathrm{CO_2}]/[\mathrm{CO_2}]_0\right)/\ln(2) \end{aligned} \qquad \textbf{[S2]}$$

$$R_{\mathrm{CH_4}} = 0.036\ \left(\sqrt{[\mathrm{CH_4}]} - \sqrt{[\mathrm{CH_4}]_0}\right) \qquad \textbf{[S3]}$$

$$R_{\mathrm{N_2O}} = 0.12\ \left(\sqrt{[\mathrm{N_2O}]} - \sqrt{[\mathrm{N_2O}]_0}\right), \qquad \textbf{[S4]}$$

where the subscript "0" refers to preindustrial concentrations. Note that the greenhouse effect due to changes in water vapor is part of the fast feedbacks and is hence not included here. For a given emission scenario (4), $C_{\mathrm{CO_2}}$ was calculated using LOSCAR. $C_{\mathrm{CH_4}}$ and $C_{\mathrm{N_2O}}$ were determined from:

$$\mathrm{d}C_n/\mathrm{d}t = \left(C_n^0 - C_n\right)/\tau_n^* + F_n, \qquad \textbf{[S5]}$$

where C^0, τ^*, and F are preindustrial concentrations, mean lifetimes ($\tau^*_{\mathrm{CH_4}} = 12$ y, $\tau^*_{\mathrm{N_2O}} = 114$ y; refs. 11, 12), and emissions, respectively. $F_{\mathrm{CH_4}}$ and $F_{\mathrm{N_2O}}$ were taken proportional to CO_2 emissions and scaled based on published GHG emission ratios (13). Anthropogenic emissions of non-CO_2 GHGs are not to be confused with slow non-CO_2 GHG feedbacks in response to warming (Table 1).

Permafrost. Carbon release from permafrost represents a feedback to the warming. However, it can be included explicitly here as a CO_2 source enhancing radiative forcing, rather than implicitly affecting λ values in a less specific fashion (*Feedback Analysis*). The permafrost carbon inventory, C_p, was determined from:

$$\mathrm{d}C_p/\mathrm{d}t = \left(C_p^{eq}(T) - C_p\right)\Big/\tau_p, \qquad \textbf{[S6]}$$

where $\tau_p = 100$ y is the permafrost response time. The equilibrium inventory is $C_p^{eq}(T) = C_p^0 - \alpha_p(T - T^0)$, where $C_p^0 = 1,700$ Pg C (ref. 14) is the carbon mass at T^0 and $\alpha_p = 50$ to 150 Pg C·K^{-1} represents the sensitivity of the reservoir size to warming (14–16). The present standard simulation assumes a small sensitivity of $\alpha_p = 50$ Pg C·K^{-1}.

Oceanic Hydrates. Carbon release from oceanic methane hydrates can also be included explicitly as a carbon source. The change in carbon mass of the oceanic hydrate reservoir was calculated from:

$$\mathrm{d}M/\mathrm{d}t = -\left(M_f - M_f^{eq}\right)\Big/\tau_f, \qquad \textbf{[S7]}$$

with $M_f^{eq} = x_f\ C^0\ e^{-0.55\Delta T}$ (ref. 17), where $x_f = 0.4$ is the fraction of the reservoir available for dissociation on timescales $\lesssim 10^4$ y (subscript f). The factor "0.55" in the exponential means that the reservoir size drops to $1/e$ for a temperature increase of $\Delta T = 1/0.55 \sim 1.8$ K, where ΔT is the warming above preindustrial levels (17). Furthermore, τ_f = 5,000 y is the response time and C^0 = 2,000 Pg C is the initial carbon mass. The fraction of the reservoir that is stable for $t \lesssim 10^4$ y is $M_s = (1 - x_f)C^0$ and $M = M_f + M_s$. Note that C^0 = 2,000 Pg C (18) used here is less than one-half of the initial inventory of 5,000 Pg C assumed in ref. 17, resulting in a moderate future warming contribution from methane hydrate dissociation.

Ocean Heat Uptake Efficiency. Ocean heat uptake efficiency is known to delay surface warming over a few centuries (19–21) and was explicitly included here. During heat storage, we may write $\Delta T = (\Delta R_f - N)S(t)$, where $N = C^* \mathrm{d}(\Delta T)/\mathrm{d}t$ and C^* is an effective heat capacity (1, 20, 22). Hence $\mathrm{d}(\Delta T)/\mathrm{d}t = [\Delta R_f - \Delta T/S(t)]/C^* = [S(t)\Delta R_f - \Delta T]/\tau_s$, where $\tau_s = S(t)\cdot C^*$ is a surface response time. This expression is readily integrated if a value for C^* is assumed. C^* and τ_s are not constant but increase substantially over time due to ocean mixing processes (21, 22). Thus, a time-dependent $C^*(t)$ was used here ($\Delta T \neq 0$):

$$\tau_s = S(t)\cdot C^*(t) = S(t)\left[C_0^* + \left(C_\infty^* - C_0^*\right)\overline{\Delta T}/\Delta T\right], \qquad \text{[S8]}$$

where C_0^* and C_∞^* were chosen so that $\tau_s^0 = 20$ y and $\tau_s^\infty = 1,000$ y for $S = const.$ as $t \to 0$ and $t \to \infty$, respectively. $\overline{\Delta T}$ was determined using (see *Main Text*):

$$\overline{\Delta T}_j = (2\tau_j)^{-1} \int_{t-2\tau_j}^{t} \Delta T(t')dt' \qquad \text{[S9]}$$

with an integration time of 300 y. These parameter choices resulted in ~83% and ~97% surface response to instant CO_2 doubling at 100 y and 1,000 y, respectively, slightly faster than the intermediate climate response function of Hansen et al. (21). With this setup, the present LOSCAR model runs also showed reasonable agreement with observed and predicted 20th- and 21st-century warming.

Deep-Sea Sediments and Chemical Weathering. On timescales $>10^2$ y, fossil fuel CO_2 neutralization involves reaction with $CaCO_3$ in deep-sea sediments and enhanced weathering (3, 23, 24). These processes represent slow, negative carbon cycle feedbacks that tend to reduce atmospheric CO_2 levels and are included explicitly in the carbon cycle model LOSCAR (3) (Table 1).

Illustration of Ice Sheet Feedback Parameter

An illustration of the ice sheet feedback parameter used in the future projections (see *Main Text*) is given below. It is emphasized that the following is merely an illustration—a rigorous analysis of the ice–albedo feedback is substantially more complex.

Consider the short-wave radiation term $Q(1-\alpha)$ in a planetary energy balance, where α is the albedo and $Q = S_0/4$, with S_0 being the solar constant. If only the effect of land ice sheets on albedo is considered (index L), the change of this term with temperature represents the change in radiative flux due to albedo changes ($\Delta R_L/\Delta T$, Eq. **1**). Hence $\mathrm{d}[Q(1-\alpha)]/\mathrm{d}T$ may be interpreted as the land ice feedback parameter (25):

$$\frac{\Delta R_L}{\Delta T} = \frac{\mathrm{d}[Q(1-\alpha)]}{\mathrm{d}T} = -Q\ \frac{\mathrm{d}\alpha}{\mathrm{d}T} = \lambda_L. \qquad \text{[S10]}$$

Assuming a simple representation of albedo:

$$\alpha = f_L\alpha_L + (1-f_L)\alpha_R, \qquad \text{[S11]}$$

where f_L is the area fraction covered by land ice, and α_L and α_R are the albedo of land ice and the remaining area, respectively (both independent of T), we have:

$$\frac{\mathrm{d}\alpha}{\mathrm{d}T} = \frac{\mathrm{d}f_L}{\mathrm{d}T}\ (\alpha_L - \alpha_R). \qquad \text{[S12]}$$

Using Eq. **S10** yields:

$$\frac{\mathrm{d}f_L}{\mathrm{d}T} = -\frac{\lambda_L}{Q\ (\alpha_L - \alpha_R)}\ . \qquad \text{[S13]}$$

In this simple model, the change in areal land ice cover is therefore directly proportional to λ_L. For example, for the Last Glacial Maximum (LGM)–Holocene transition, λ_L may be taken as $0.70\ \mathrm{W\cdot m^{-2}\cdot K^{-1}}$ (25, 26). Furthermore, assume that a global LGM–Holocene temperature rise of 5.8 K was accompanied by a $17 \times 10^{12}\ \mathrm{m^2}$ reduction in land ice cover (North American and Eurasian ice sheets) (26). Hence, using the proportionality between λ_L and ice cover changes (Eq. **S13**), a λ_L of 0.05 $\mathrm{W\cdot m^{-2}\cdot K^{-1}}$ as applied in the moderate future scenario would correspond to a change in land ice cover of $1.2 \times 10^{12}\ \mathrm{m^2}$. This number represents ~8% of the present combined ice cover in Greenland and Antarctica. Thus, in analogy to the LGM–Holocene transition, after >5,000 y into the future, a 5.8 K warming would reduce high-latitude ice sheet cover by ~8% in the moderate future scenario (Fig. 2). Again, these numbers need to be taken with caution because the above is just an illustration based on a simple model. Nevertheless, it is noted that the warming threshold for irreversible deglaciation of the Greenland ice sheet has been estimated at 3.1 and 1.6 K above preindustrial levels (27, 28).

Mean Warming Index

The mean warming index for projection i defined in the *Main Text* is:

$$W_i = (t_2 - t_1)^{-1} \int_{t_1}^{t_2} \Delta T_i(t)\ dt, \qquad \text{[S14]}$$

where $\Delta T_i(t)$ is the global surface warming above preindustrial levels; $[t_1, t_2] = [\mathrm{Y2013, Y10000}]$. Thus, W_i represents the calculated average future warming from the present until year 10,000. For the present simulations, W_i predominantly measures the longevity of the warming because the projections show a long warming tail, rather than intense peak warming followed by rapid cooling (Fig. S1). If the latter was true, intense/short-lived warming could produce the same average warming as less intense/long-lived warming. However, the present simulations do not show intense/short-lived warming (Fig. S1).

Regarding the warming threshold for the irreversible deglaciation of the Greenland ice sheet, the timescale of melt depends strongly on the magnitude and duration of the temperature overshoot above the threshold (27, 28). This feature is better represented here by W_i (Eq. **S14**) than by the maximum warming. For example, all but one simulation with $W_i > 3.1$ K also include sustained warming $\Delta T > 3.1$ K for more than 4,000 y (Fig. S1). The temperature anomaly for the projection with 2,000 Pg C and $\sum \lambda_j^{es} = 0.12\ \mathrm{W\cdot m^{-2}\cdot K^{-1}}$ (green line) shows a slightly shorter duration above 3.1 K. However, this is partly compensated for by a larger overshoot above the threshold of 3.1 K (maximum $\Delta T = 4.5$ K).

Silicate Weathering and Final Equilibrium

On timescales of 10^5 to 10^6 years following the onset of a perturbation (e.g., GHG release), equilibrium will finally be restored in the coupled carbon cycle–climate system. This assumes absence of any other external perturbation, no changes in boundary conditions, orbital forcing, etc. Under a continued, sustained forcing, the final equilibrium would be different from the initial equilibrium before the perturbation. If the forcing disappears over time, then the final and initial equilibrium would be equal. Within the current framework, these two situations may be illustrated by varying the strength of the silicate weathering feedback in the model (Fig. S2).

Enhanced silicate weathering and subsequent carbonate burial ultimately removes excess carbon from the ocean–atmosphere system. The silicate weathering feedback in LOSCAR is parameterized based on (3, 6, 29–31):

$$F_{si} = F_{si}^0 \left(pCO_2 / pCO_2^0 \right)^{n_{si}}, \quad \textbf{[S15]}$$

where the superscript "0" refers to the initial (steady-state) value of the weathering flux and pCO_2, respectively. The parameter n_{si} controls the strength of the weathering feedback. For example, for $n_{si} = 0$ there is no silicate weathering feedback; F_{si} is constant, only the carbonate weathering feedback is active (3). The carbon that has been added to the exogenic carbon cycle would accumulate in the surface reservoirs, part of which would remain in the atmosphere. This causes a sustained forcing that remains constant after several 10 thousand years (Fig. S2; $n_{si} = 0$). This example illustrates the system's approach to the final equilibrium under a sustained forcing. The final equilibrium surface temperature is elevated relative to the initial value.

For $n_{si} > 0$, the enhanced silicate weathering flux and subsequent carbonate burial removes carbon from the ocean–atmosphere system as long as the partial pressure of atmospheric CO_2 remains higher than the initial pCO_2^0. The timescale of restoring the final equilibrium via silicate weathering is probably of the order of 500 ky to 1 My but is uncertain because of uncertainties in the weathering parameterization. Typical values assumed for n_{si} may range from 0 to 0.6 (6, 32) (Fig. S2); the standard value used in the present LOSCAR simulations is 0.2 (*Main Text*). The case for $n_{si} > 0$ illustrates the system's approach to the final equilibrium when the forcing disappears over time. The initial and final equilibrium surface temperatures are equal. Again, this scenario only applies in the absence of any other external perturbation/forcing, no changes in boundary conditions, orbital parameters, etc.

1. Roe G (2009) Feedbacks, timescales, and seeing red. *Annu Rev Earth Planet Sci* 37:93–115.
2. Zeebe RE, Zachos JC, Dickens GR (2009) Carbon dioxide forcing alone insufficient to explain Palaeocene-Eocene Thermal Maximum warming. *Nat Geosci* 2:576–580, 10.1038/ngeo578.
3. Zeebe RE (2012) LOSCAR: Long-term Ocean-atmosphere-Sediment CArbon cycle Reservoir Model v2.0.4. *Geosci Model Dev* 5:149–166.
4. Zeebe RE, Zachos JC, Caldeira K, Tyrrell T (2008) Oceans. Carbon emissions and acidification. *Science* 321(5885):51–52, 10.1126/science.1159124.
5. Zachos JC, Dickens GR, Zeebe RE (2008) An early Cenozoic perspective on greenhouse warming and carbon-cycle dynamics. *Nature* 451(7176):279–283, 10.1038/nature06588.
6. Uchikawa J, Zeebe RE (2008) Influence of terrestial weathering on ocean acidification and the next glacial inception. *Geophys Res Lett* 35:L23608, 10.1029/2008GL035963.
7. Stuecker MF, Zeebe RE (2010) Ocean chemistry and atmospheric CO_2 sensitivity to carbon perturbations throughout the Cenozoic. *Geophys Res Lett* 37:L03609, 10.1029/2009GL041436.
8. Komar N, Zeebe RE (2011) Changes in oceanic calcium from enhanced weathering did not affect calcium-based proxies during the Paleocene-Eocene Thermal Maximum. *Paleoceanography*, 10.1029/2010PA001979.
9. Zeebe RE (2012) History of seawater carbonate chemistry, atmospheric CO_2, and ocean acidification. *Annu Rev Earth Planet Sci* 40:141–165.
10. Myhre G, Highwood EJ, Shine KP, Stordal F (1998) New estimates of radiative forcing due to well mixed greenhouse gases. *Geophys Res Lett* 25:2715–2718.
11. Intergovernmental Panel on Climate Change (2007) *Climate Change 2007: The Physical Science Basis*, eds Solomon S, et al. (Cambridge Univ Press, Cambridge, UK).
12. Solomon S, et al. (2010) Persistence of climate changes due to a range of greenhouse gases. *Proc Natl Acad Sci USA* 107(43):18354–18359.
13. Intergovernmental Panel on Climate Change (2000) *Special Report Emissions Scenarios*, eds Nakicenovic N, Swart R (Cambridge Univ Press, Cambridge, UK), p 570.
14. Schaefer K, Zhang T, Bruhwiler L, Barrett AP (2011) Amount and timing of permafrost carbon release in response to climate warming. *Tellus B Chem Phys Meterol* 63:165–180.
15. Schuur EAG, Abbott B (2011) Climate change: High risk of permafrost thaw. *Nature* 480(7375):32–33.
16. Schneider von Deimling T, et al. (2012) Estimating the near-surface permafrost-carbon feedback on global warming. *Biogeosciences* 9:649–665.
17. Archer D, Buffett B (2005) Time-dependent response of the global ocean clathrate reservoir to climatic and anthropogenic forcing. *Geochem Geophys Geosyst* 6:3002.
18. Archer D, Buffett B, Brovkin V (2009) Ocean methane hydrates as a slow tipping point in the global carbon cycle. *Proc Natl Acad Sci USA* 106(49):20596–20601.
19. Hansen J, et al. (1985) Climate response times: Dependence on climate sensitivity and ocean mixing. *Science* 229(4716):857–859.
20. Gregory JM, Forster PM (2008) Transient climate response estimated from radiative forcing and observed temperature change. *J Geophys Res* 113(D12):D23105.
21. Hansen J, Sato M, Kharecha P, von Schuckmann K (2011) Earth's energy imbalance and implications. *Atmos Chem Phys* 11:13421–13449.
22. Watterson IG (2000) Interpretation of simulated global warming using a simple model. *J Clim* 13:202–215.
23. Archer D (2005) Fate of fossil fuel CO_2 in geologic time. *J Geophys Res* 110(1012):C09S05, 10.1029/2004JC002625.
24. Ridgwell AJ, Hargreaves JC (2007) Regulation of atmospheric CO_2 by deep-sea sediments in an Earth system model. *Global Biogeochem Cycles*, 10.1029/2006GB002764.
25. Rohling EJ, et al. (2012) Making sense of palaeoclimate sensitivity. *Nature* 491(7426):683–691, 10.1038/nature11574.
26. Köhler P, et al. (2010) What caused Earth's temperature variations during the last 800,000 years? Data-based evidence on radiative forcing and constraints on climate sensitivity. *Quat Sci Rev* 29:129–145.
27. Gregory JM, Huybrechts P (2006) Ice-sheet contributions to future sea-level change. *Philos Trans A Math Phys Eng Sci* 364(1844):1709–1731.
28. Robinson A, Calov R, Ganopolski A (2012) Multistability and critical thresholds of the Greenland ice sheet. *Nat Clim Change* 2:429–432.
29. Walker JCG, Hays PB, Kasting JF (1981) Negative feedback mechanism for the long-term stabilization of earth's surface temperature. *J Geophys Res* 86:9776–9782.
30. Berner RA, Lasaga AC, Garrels RM (1983) The carbonate-silicate geochemical cycle and its effect on atmospheric carbon dioxide over the past 100 million years. *Am J Sci* 283:641–683.
31. Walker JCG, Kasting JF (1992) Effects of fuel and forest conservation on future levels of atmospheric carbon dioxide. *Global Planet Change* 97:151–189.
32. Tyrrell T, Shepherd JG, Castle S (2007) The long-term legacy of fossil fuels. *Tellus B Chem Phys Meterol* 59:664–672.

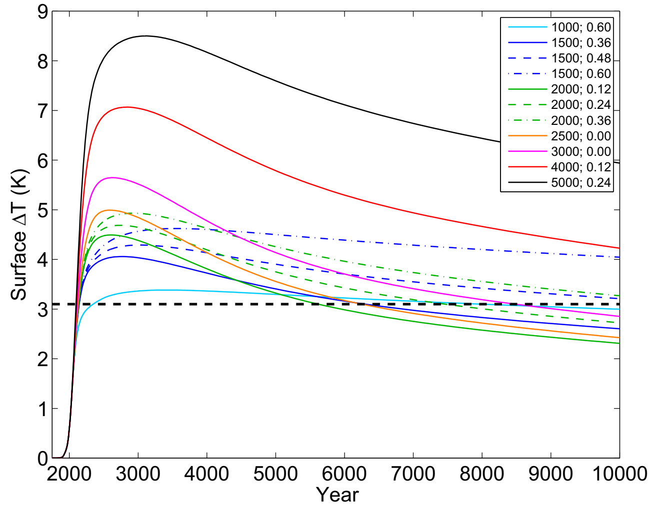

Fig. S1. Selected future warming projections with $W_i > 3.1$ K (Fig. 3). The numbers in the legend indicate total carbon input (in petagrams of carbon); $\sum \lambda_j^{es}$ (in watts per square meter per kelvin). The horizontal dashed line indicates the warming threshold of 3.1 K given in ref. 1 for the irreversible deglaciation of the Greenland ice sheet.

1. Gregory JM, Huybrechts P (2006) Ice-sheet contributions to future sea-level change. *Philos Trans A Math Phys Eng Sci* 364(1844):1709–1731.

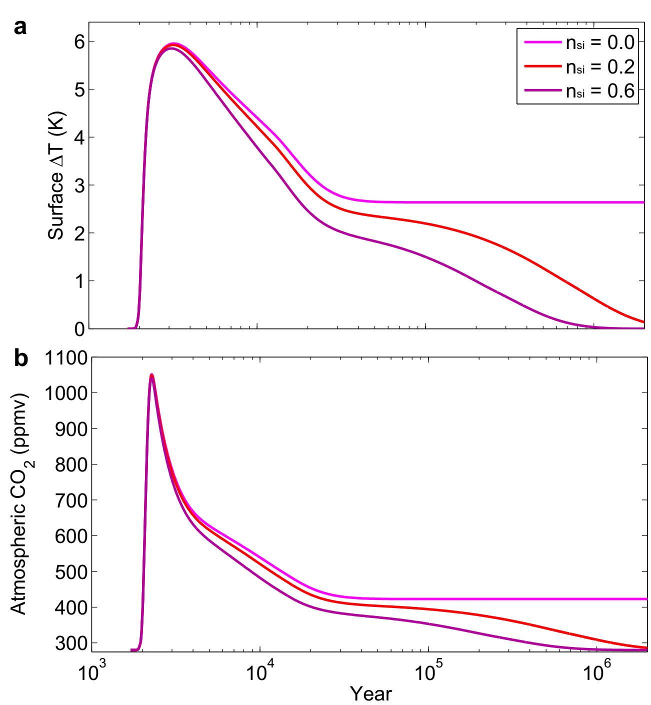

Fig. S2. Illustration of the system's approach to final equilibrium. (*A*) Global surface temperature anomaly and (*B*) atmospheric CO_2 concentration. The graphs indicate three different strengths of the silicate weathering feedback (see text). Moderate slow-feedback parameters and carbon emissions of 2,500 Pg C over 500 y were used in all three scenarios (Fig. 2).